WSRL-GD-28/90

AR-006-450

AD-A230 872

BASIC RHEOLOGY AND ITS APPLICATION TO NITROCELLULOSE PROPELLANT PROCESSING BY SCREW MIX-EXTRUDERS

R.C. WARREN

ORDNANCE SYSTEMS DIVISION

WEAPONS SYSTEMS RESEARCH LABORATORY

DTIC
S ELECTE
E JAN 29 1991
D

Approved for Public Release.

SEPTEMBER 1990

91 1 28 0 0

DSTO AUSTRALIA

GENERAL DOCUMENT
WSRL-GD-28/90

BASIC RHEOLOGY AND ITS APPLICATION TO NITROCELLULOSE PROPELLANT PROCESSING BY SCREW MIX-EXTRUDERS

R.C. Warren

S U M M A R Y (U)

This document is intended to provide an introductory review of the rheology of propellant doughs and the propellant mixing process. The fundamental rheological quantities describing the flow of propellant doughs in mixing and extrusion are described, and the molecular factors affecting flow are discussed. Batch mixing is analysed in terms of the fundamental parameters which have been introduced, and a method of analysing screw mix-extrusion in a similar way is suggested.

Author's address:
    Ordnance Systems Division
    Weapons Systems Research Laboratory
    PO Box 1700, Salisbury
    South Australia

Requests to: Chief, Ordnance Systems Division

Accession For	
NTIS GRA&I	☒
DTIC TAB	
Unannounced	☐
Justification	
By	
Distribution/	
Availability Codes	
Dist	Avail and/or Special
A-1	

TABLE OF CONTENTS

LIST OF FIGURES

1. INTRODUCTION

The rheology of filled and unfilled nitrocellulose (NC) doughs is a subject of particular interest at the present time because of the push both overseas and locally away from batch propellant manufacturing processes to continuous processes. NC is unlike most of the polymers processed to date in the plastics and rubber industries. In its raw state NC retains much of the supermolecular structure of the precursor cellulose, and it exists in the form of fibres. The object of propellant processing is to transform the fibrous NC into a consolidated solid, which can be shaped directly into propellant grains or used as a binder for solid filled propellants.

Much of the knowledge gained from "hands-on" experience of the old batch processes may no longer be relevant, and new concepts, based on an understanding of rheology, may be required to describe the new processes. This General Document is intended to provide an introduction to rheology, and to demonstrate its relevance to the development of new propellant manufacturing processes. In Section 2 the fundamental rheological quantities which are relevant to the flow of propellant doughs in mixing and extrusion are described. These factors include shear rate, shear stress, shear and extensional viscosities, and modulus. A brief discussion of the physical behaviour of polymer molecules and the way the molecular factors increase elasticity and viscosity is given. Many propellants are highly filled with finely ground energetic solids, and the general effects of solid fillers on flow behaviour are discussed. The final effect to be considered is viscous heat generation. Heat is generated when viscous materials are deformed, and at high deformation rates this heating can lead to large increases in temperature and corresponding decreases in viscosity.

Section 3 is devoted to mixing processes. Batch mixing in an incorporator, which is the current method of manufacturing most gun propellants, is analysed in terms of both readily observable parameters and fundamental parameters. Methods of calculating scale-up factors from small to large mixers are discussed, and models of rubber and NC propellant mixing are reviewed. The mixing processes occurring in a screw mix-extruder (SME) are analysed in a similar way to those occurring in the batch process. The concept of a residence time distribution is introduced as a method of monitoring the degree of mixing occurring in the SME. Methods for calculating the capacity for conveying screws to generate pressure for extrusion are indicated, and a theory of devolatilisation of volatile solvents is discussed.

Much of the basic information in this document is covered in varying degrees of depth in a number of good text books or review articles(ref.1 to 7), and specific references to these will not be given. However, for more recent or more detailed information, which is not covered in text books, specific references will be given to the appropriate literature.

2. BASIC RHEOLOGY

2.1   General

This section will introduce those rheological concepts which are relevant to propellant processing. The discussion is intended only to give an intuitive understanding of the flow behaviour of propellant

doughs during mixing and extrusion. It is not intended to be a complete treatment, as there are many excellent text books which give detailed discussions of this subject(ref.1 to 7).

2.2   Shear flow

2.2.1   *Shear stress, shear rate and viscosity*

The most widely used flow parameter is shear viscosity. However, it is important to remember that shear viscosity is only defined for a certain class of simple flows called viscometric flows, ie flows where viscosity can be measured. Viscometric flows are essentially uniform flows where the particles of the material undergo steady shear flow independent of time. The relevant rheological parameters are shear stress and shear rate, and these will be introduced by considering drag flow between two flat parallel plates moving relative to each other, with the bottom plate stationary, see figure 1. Shear stress is defined as the force acting on the plates divided by the area of the plates, ie

$$\tau = F/A,$$

where F is the force and A is the area. Shear strain, γ, is defined as the distance moved by the top plate divided by the plate separation. Hence the rate of change of shear strain, or shear rate, $\dot{\gamma}$, is the velocity of the plate divided by the separation, ie

$$\dot{\gamma} = V/h,$$

where V is the velocity of the top plate, and h is the separation.

An equivalent flow occurs in the annular gap between 2 concentric cylinders in relative rotation at angular velocity Ω about their common axis, see figure 2. The diameters of the inner and outer cylinders are R and Ro respectively, and it is assumed that a torque, T, is measured at the inner cylinder. The shear stress on the surface of the inner cylinder is given by:

$$\tau = T/(2\pi R^2 L),$$

where L is the length of the cylinders. If the fluid is Newtonian, the shear rate can be calculated from the angular rotation rate, Ω, by

$$\dot{\gamma} = 2\Omega/(1 - s^2),$$
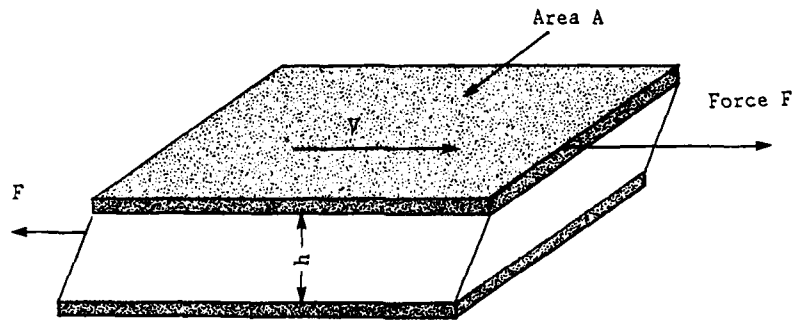
Figure 1. Simple shear flow between parallel plates
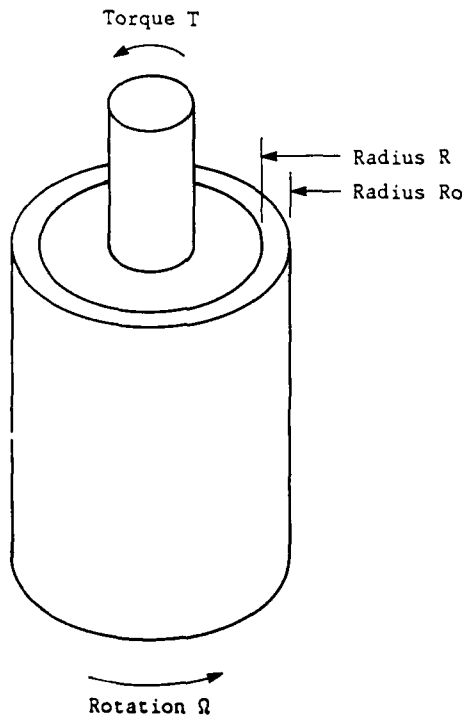
Figure 2. Couette flow geometry

where s = R/Ro. However, for non-Newtonian fluids the calculation of $\dot\gamma$ is more complicated. This geometry is known as Couette flow, and is similar to the flow occurring at the tip of blades in propellant incorporators.

Pressure driven flow in a pipe or capillary is also a viscometric flow. In this case the flow is telescopic, consisting of cylindrical layers sliding past one another. At the wall of the pipe, the shear flow can be analysed by considering a shell of infinitesimal thickness dr and length L, as defined in figure 3. The pressure to drive the flow is assumed to be P at one end of the capillary and zero at the other. The viscous force on the shell equals the average pressure in the capillary P/2, times the cross-sectional area of the capillary, ie

$$F = 2\pi R^2 P/2,$$

and the area of the shell is

$$A = 2\pi R.L$$
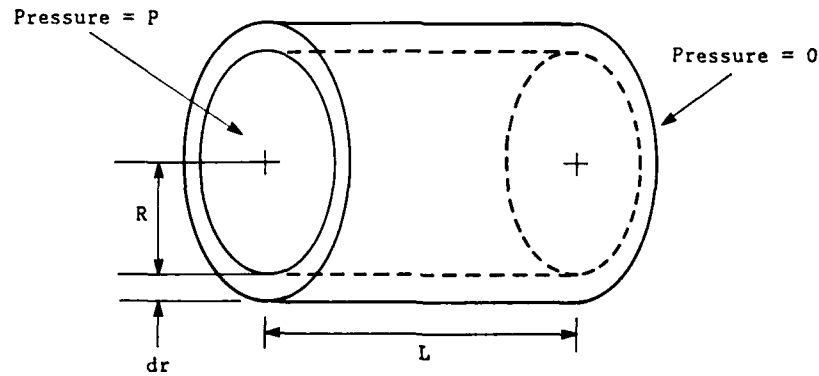
Figure 3. Shear flow in a pipe or capillary

The force generated by the pressure drop must be resisted by the shear stress on the shell, therefore the shear stress on the shell surface is

$$\tau_w = \frac{F}{A} = \frac{\pi R^2 P}{2 R L} = \frac{PR}{2L}$$

A rigorous derivation gives the same result for the stress at the wall, and also shows that the radial variation of stress in a pipe or capillary is given by;

$$\tau = \frac{Pr}{2L} = \frac{\tau_w r}{R}$$

This is an important result, because it shows that in any pipe flow the shear stress varies linearly along the radius from zero at the centre to a maximum at the wall. This property can be useful in estimating the way the shear rate changes with radius from a knowledge of the viscosity.

The second rheological quantity that can be calculated is the shear rate, which is defined as the velocity gradient dV/dr. V is the fluid velocity in the axial direction at a radial distance r. The velocity gradient at the wall is proportional to the average velocity gradient, ie

$$\dot{\gamma} = \frac{dV}{dr} \sim \frac{V^*}{R},$$

where

$$V^* = \frac{Q}{\pi R^2}.$$

Therefore

$$\dot{\gamma} \sim \frac{Q}{\pi R^3}$$

where Q is the volume flow rate. For a Newtonian fluid with constant viscosity η, exact calculation gives

$$\dot{\gamma} = \frac{4Q}{\pi R^3},$$

and

$$\tau = \eta \dot{\gamma}$$

Many low molecular weight fluids are Newtonian, which means that the shear stress increases in strict proportion with increasing shear rate. The molecules of these fluids interact strongly only with nearest neighbours, so that flow occurs by individual molecules sliding past each other. However, polymeric materials, including NC, consist of long chainlike molecules which entangle with each other. See Section 2.5.1 for a discussion of molecular structure. At very low shear rates many polymeric materials are Newtonian, because there is sufficient time for them to adjust their configuration in response to the deformation. However, at moderate and high shear rates, the stresses which are generated alter the configuration of the molecules in such a way as to reduce resistance to flow. Hence the viscosity decreases with increasing shear rate, and as a result the shear stress increases at a lower rate than strict proportionality to shear rate. This phenomenon is known as pseudoplasticity or shear thinning.

If the shear stress of a pseudoplastic material is plotted vs shear rate on a log-log plot similar to figure 4, the curve is linear over a wide range of shear rates. The slope of the curve is less than 1, whereas the slope on a Newtonian fluid equals 1. The curve can be described by a power law:

$$\tau = k.\dot{\gamma}n$$

where k is the consistency index, and n is the power law exponent. These 2 parameters are sufficient to characterise the shear flow of many polymers.

The symmetry of the flow in a pipe or capillary dictates that shear stress and shear rate are zero at the centre, and that they increase monotonically to maximum values at the wall. The velocity profile, which is the integral of the shear rate profile, is determined by the form of the dependence of shear stress on shear rate. For Newtonian fluids the velocity profile is parabolic, see figure 5. However, pseudoplastic fluids have less resistance to flow at high shear rates than for Newtonian fluids, so the maximum value of shear rate will be higher for the same volume flow rate. Hence the velocity profile will be steeper at the wall, and correspondingly flatter in the centre of the flow, as illustrated in figure 5. The lower the value of n, the further the profile deviates from a parabola, and the more pluglike the flow becomes.
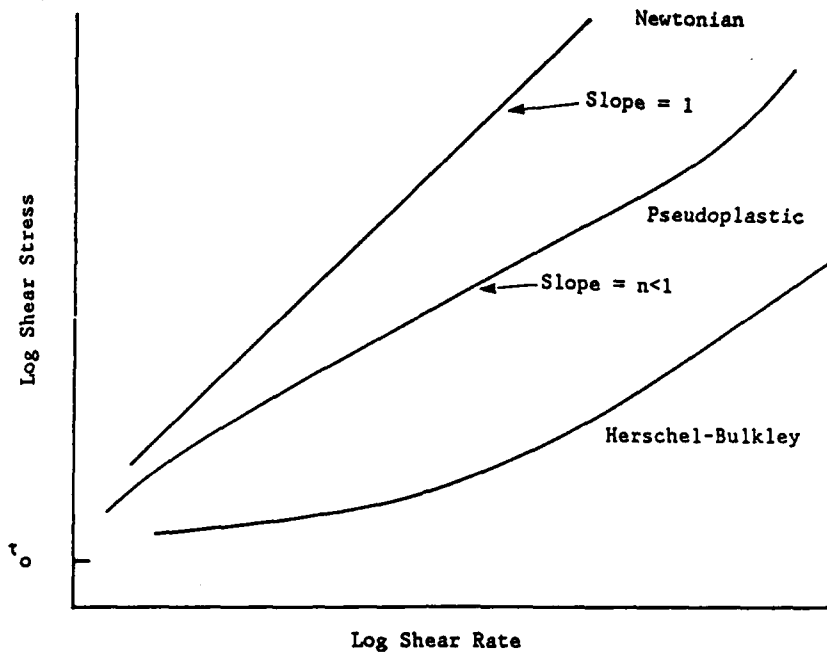
Figure 4. Flow curves of various types of fluids
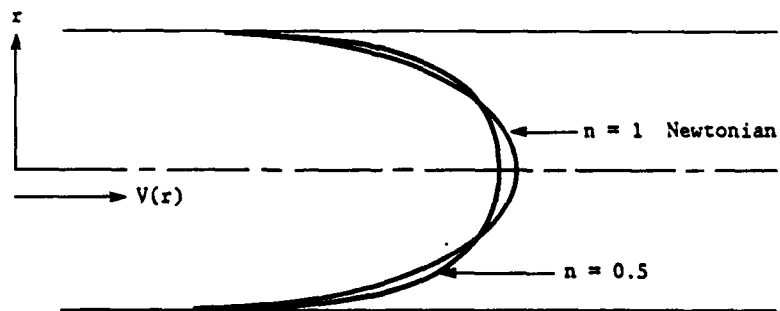
Figure 5. Flow velocity profiles of a Newtonian and power law fluid in a pipe

The steeper velocity gradient at the wall for fluids with n < 1 means that the true shear rate at the wall will be greater than the Newtonian value calculated from $\dot{\gamma} = 4Q/\pi R^3$, which is called the apparent shear rate. The true shear rate at the wall can be obtained from the apparent shear rate by applying a correction factor.

A property of NC doughs which is not shared by many other types of unfilled polymers is a yield stress for flow. The existence of a yield stress means that a critical stress, τ_0, must be exceeded before flow can occur. The effect of a yield stress on the flow curve is illustrated schematically in figure 4, where it can be seen that there is considerable curvature of the flow curve at low shear rates as the stress tends to the yield value, τ_0. The flow curve can be fitted by the Herschel-Bulkley equation:

$$\tau = \tau_0 + k\dot{\gamma}^n$$

The yield stress has effects in both extrusion and mixing. In capillary flow, a yield stress causes the material at the centre of the flow, where the shear stress is below the yield value, to travel as an unsheared plug. The yield stress also has an effect on the efficiency of mixing in an incorporator, where lumps of undeformed material will circulate in low stress regions where the local stress does not exceed the yield stress.

As is typical of materials with a yield stress, NC doughs also display thixotropy. A thixotropic material is one whose viscosity depends explicitly on the duration of the shearing. Both yield stress and thixotropy are due to a structure in a material which has to be broken down before flow can occur. Many highly filled materials and suspensions are thixotropic because the filler particles agglomerate to form rigid networks. However, some other explanation must apply to the thixotropy of unfilled NC doughs. It is believed that they have a cholesteric liquid crystal structure, in common with many other cellulosic materials(ref.8). It has been postulated that thermal fluctuations in the layers of the structure are responsible for the yield stress.

Whatever the detailed mechanism of thixotropy may be in particular cases, its effect in general can be visualised in the following way. At the beginning of flow only small stresses are generated, and the structure need only be slightly disturbed to allow flow. However, at longer times the structure breaks down further into smaller units, which slide more easily past each other. The progressive breakdown of the structure takes time, and hence the viscosity is time dependent. When the flow ceases, the structure usually reforms, but the rate of reformation is usually much less than the rate of breakdown.

The main effect of thixotropy on NC propellant processing behaviour is the phenomenon of stress overshoot. If a deformation is applied at a rate greater than can be accommodated by the dynamics of structure breakdown, the stress will overshoot and then decay to the equilibrium value as the structure appropriate to the applied deformation rate develops.

Thixotropy may be important in propellant extrusion, where the time the dough spends in the die is short, and the flow is essentially transient. The magnitude of the effect of thixotropy has not been studied in detail to date because of experimental difficulties and the lack of a suitable theoretical framework. The effect may not be too severe in practice because the dough passes through sieves and screens before entering the die, and much of the structure may be broken down there. If the transit time through the sieves and dies is short enough, the structure may not reform in time to affect extrusion behaviour.

A second situation where thixotropy may be important is in the flow in the gap between the blade tip and the wall in the incorporator. The propellant dough spends much of the time in the low stress regions of the mixer, but periodically it is caught up by the blade and squeezed through the gap (see Section 3 for more details of mixing). The transient nature of the flow through the gap suggests that thixotropy may play a role, and that the stresses generated may be higher than would be calculated from steady state flow. This effect has been noted for rubber (reference 9, page 938).

2.2.2   Wall slip

In the discussion so far it has been assumed that the fluid adheres to the boundaries of the flow, and in particular to the walls in pipe or capillary flow. However, in some circumstances the observed flow behaviour indicates that some form of slip occurs at the wall. In propellant doughs, if slip occurs, it is likely to be due to the migration of low molecular weight species to the wall to form a lubricating film. At low shear rates the lubrication can significantly reduce extrusion stresses. However, as the lubricant is of low molecular weight, its viscosity is Newtonian, and as the shear rate increases, the shear stress in the layer would increase more rapidly than the shear stress in the bulk of the fluids which is pseudoplastic. Hence the lubrication would be less effective at high shear rates.

The effect of wall slip on flow curves is illustrated schematically in figure 6. Above a certain shear stress where the slip is initiated, the shear stress deviates from the no-slip curve. The amount of deviation is dependent on capillary diameter. For small diameters the surface area to volume ratio is large, and the wall effects are correspondingly large. As the diameter increases the surface area to volume ratio drops, the effect of slip decreases, and the flow curves move closer to the no-slip curve, as illustrated in figure 6. The dependence of wall slip on capillary diameter can be used to identify and quantify wall slip.

A different type of slip behaviour has been identified in the flow of nitrocellulose propellants. In this case the "slip" is an apparent slip caused by the fundamental molecular properties of nitrocellulose(ref.10).
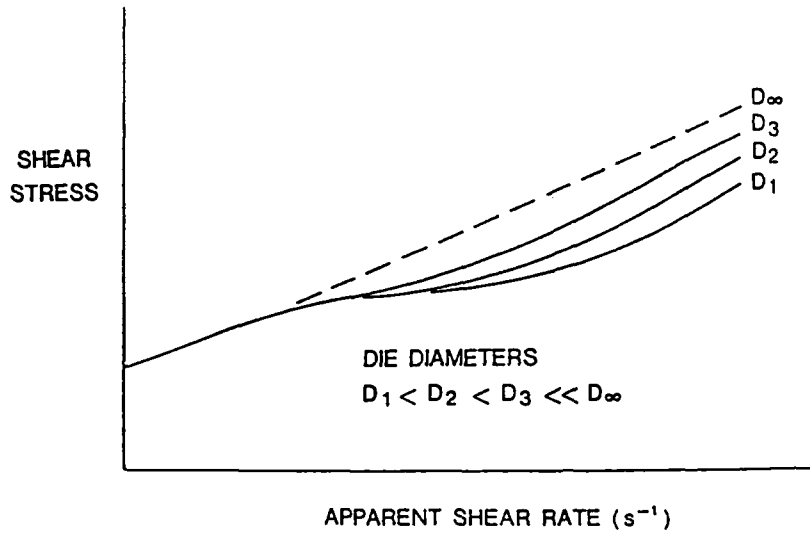
Figure 6. Schematic representation of flow curves showing the effects of wall slip

2.3   Extensional flow

A second type of flow where a unique viscosity can be defined is elongational, or extensional, flow. The simplest example is the stretching of a rod of material, as illustrated in figure 7. The elongational strain, ε, is the increase in the length of the rod, dl, divided by the instantaneous length of the rod, l, ie

$$\varepsilon = dl/l.$$

The rate of change of strain, $\dot{\varepsilon}$, is given by

$$\dot{\varepsilon} = \frac{dl}{dt} / l = V/l \qquad \dot{\varepsilon} = \frac{dl}{dt} / l$$

The stress generated by the deformation is the force , F, divided by the cross-sectional area of the rod, ie

$$\sigma_e = F/A,$$

and the extensional viscosity is defined as

$$\eta_e = \sigma_e / \dot{\varepsilon}.$$

If the flow is steady, both the length and cross-section of the rod are changing continuously with time. In order to produce a constant strain rate, the relative velocity of the rod ends must increase exponentially with time, as the rod lengthens. The stress must be evaluated from the instantaneous value of cross-sectional area.

Area = A

v = 0   v = V

F   F

|←————————————— 1 ——————————————→|

dl
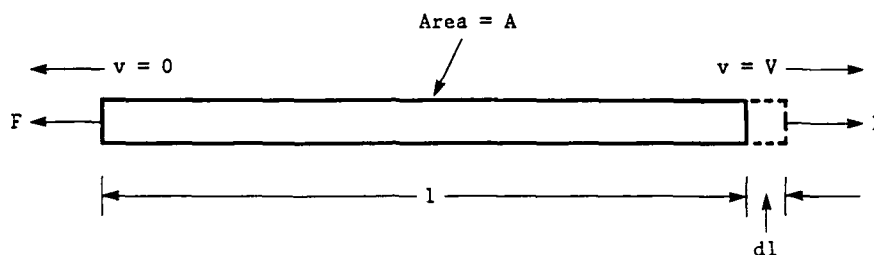
Figure 7. Extensional flow geometry

The extensional viscosity of a Newtonian fluid has been calculated by Trouton to be 3 times the Newtonian viscosity, ie

$$\eta_T = 3\eta.$$

where η_T is the so-called Trouton viscosity.

In polymeric materials undergoing deformation at very low rates, where the shear viscosity tends to Newtonian behaviour, the extensional viscosity approaches the Trouton value(ref.3). However, at higher deformation rates the shear viscosity decreases more rapidly than the extensional viscosity, which can become orders of magnitude greater than the shear viscosity. In fact the extensional viscosity for some materials increases with increasing shear rate(ref.11).

Measurement of steady state extensional viscosity at high extension rates presents serious problems because of the difficulty of maintaining a constant rate of extension for the long times required for a steady state to develop.

Probably the most common occurrence of extensional flow is in extrusion, where material is forced from a reservoir with a large diameter, through various channels of decreasing cross-section, into a small die. Since the fluid is assumed to be incompressible, the decrease in cross-sectional area imposed on the fluid can only be accommodated by an increase in length in the flow direction, ie uniaxial extension. The extension in the flow direction obviously matches the increase in linear velocity required to maintain a constant volumetric flow rate.

Extensional flow in a converging die is illustrated in figure 8. Near the die walls the flow is predominately shear, as the velocity increases rapidly from zero with distance from the wall. However, in the centre of the flow the shear is zero by symmetry and the velocity profile is flat. It can be seen that the fluid in the centre undergoes pure extension. If the walls of the die could be perfectly lubricated, the flow would be totally extensional, and an extensional viscosity could be determined from the pressure drop along the die. However, a true steady state viscosity could not be measured because the length of the die required for steady flow to develop would be prohibitively long. A further problem is the practical difficulty of ensuring adequate lubrication.
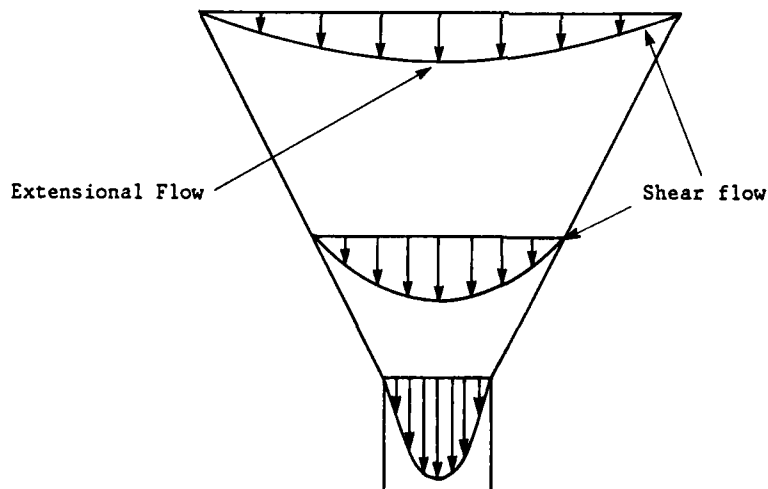
Figure 8. Extensional and shear flow in a converging die

A method of calculating an extensional viscosity from the pressure drop developed at the entrance to a capillary die has been developed by Cogswell(ref.11), but this is not a true steady state viscosity because of the short transit time involved. However, only transient extensional flows occur in propellant processing, so this method may give a viscosity which could be of use in semi-empirical analyses.

2.4   General flow geometries

In most mixing and extrusion operations, the flow geometry is complex, and it is neither wholly shear nor wholly extension. In these cases a full 2 or 3 dimensional description of the flow is required in terms of stress and strain tensors. Instead of a simple viscosity, a tensor constitutive equation is required to relate the stress tensor to strain or strain rate tensor. While 2 dimensional analyses are carried out at WSRL, they are beyond the scope of this paper.

2.5   Elasticity

2.5.1   Molecular structure

A polymer molecule is a string, or chain, of identical molecular subunits, called monomers, joined head to tail. The contour length of the chain can be hundreds or thousands of times the mean diameter (branched polymers will not be considered). Rather than form linear structures, polymer molecules tend to coil in upon themselves, see figure 9, and a random coil is often used to model the molecular structure.

The motion of real polymer molecules is very complex, and an idealised model is often used to describe their motion. A molecule is assumed to consist of a series of rigid segments, connected to neighbours at each end by flexible joints, see figure 9. The segments are assumed to be long enough to contain a number of monomers, but short enough for there to be a large number of them in each molecule. Molecular deformation occurs by these segments slipping over each other, in a similar manner to the molecular motion of low molecular weight materials.

The viscosity of the fluid as a whole can be described in terms of the friction between molecular segments(ref.12). If the force required to pull one chain segment through the rest of the fluid at unit speed is defined to be f_0, then the viscosity will be proportional to the product of the number of segments, N, and f_0, ie

$$\eta \sim N.f_0 = K.N.f_0$$

where K is a constant.

The following discussion of the flow behaviour of polymeric materials will be in general terms and based on the idealised model of molecular structure and motion. NC deviates from the ideal in a number of respects, but these deviations will be mentioned only where necessary.
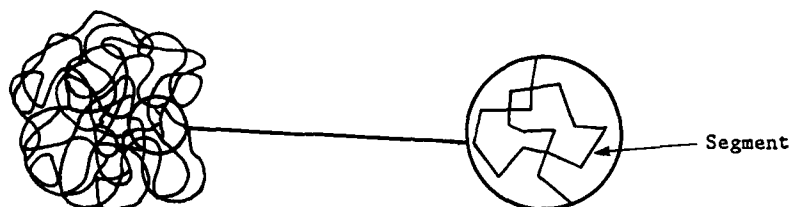
Figure 9. Schematic representation of a polymer molecule

2.5.2   *Elasticity in rubbers*

The concept of elasticity in polymers is familiar from the everyday experience of stretching rubber bands. It is instructive to examine the cause of elasticity in rubber, before considering elasticity in polymers in general.

If polymer molecules were rigid and self-contained, with no mechanism for internal deformation, they would behave in a similar manner to low molecular weight materials. At the other extreme, if the molecules were truly freely jointed, and all possible conformations were of equal energy with no entropy effects, then the forces generated by deformation would be viscous and not elastic. In order for elasticity to exist, two conditions must be satisfied. There must be a preferred low energy configuration of the molecule which leads to the generation of restoring forces if the molecule is deformed away from it, and also there must be strong intermolecular forces to transmit stress from one molecule to another.

In figure 10, a schematic representation of an idealised, non-elastic molecular structure is compared with an idealised elastic structure representative of a rubber. The inelastic structure has rigid molecules, isolated from neighbours and interacting with them through weak forces. Under an applied stress the molecules would slide past each other with only viscous resistance. In the elastic, rubbery material, stresses are transmitted between molecules through crosslinks. The crosslinks can be chemical bonds, or local areas of crystallinity which provide ties between molecules. The molecules form an infinite network, and in this way transmit the macroscopic stretching forces throughout the material. Because the chains are constrained by the crosslinks, they cannot undergo deformation indefinitely, but reach a limit which can only be exceeded by chain breakage. Hence rubbers are essentially solids, and not fluids.
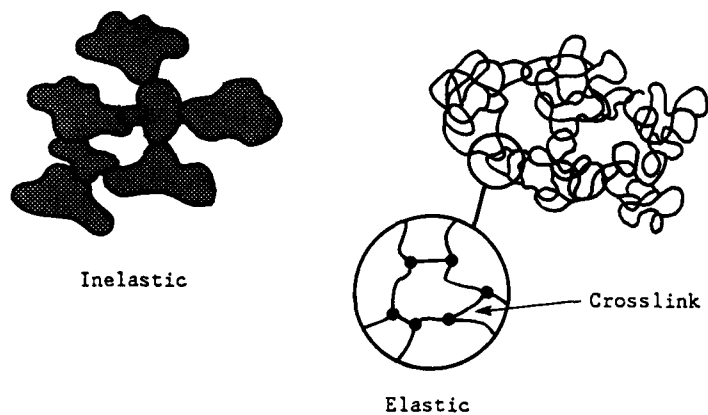
Figure 10. Schematic representation of inelastic and elastic molecular structures

There is a minimum energy configuration in rubbers which is the equilibrium state. When the rubber is deformed away from this state, a stress is generated which tends to restore the material to equilibrium. Because of the existence of an equilibrium state, rubbers have a permanent memory, and the strength of the memory depends on the density of crosslinks. For idealised rubbers, the following relations apply between stress, τ, and strain, γ or ε:

$$\tau = G\gamma \text{ for shear,}$$

and

$$\tau = \underline{E}(\exp(2\varepsilon) - \exp(-\varepsilon)) \text{ for extension,}$$

$$\approx E\varepsilon \text{ if } \varepsilon \text{ is small.}$$

where G is the shear modulus, and E is Young's, or extensional modulus. The values of the moduli depend on the crosslink density.

2.5.3   *Molecular entanglements*

An important concept in the description of molecular behaviour of polymers is the idea of an entanglement. Molecules above a critical length behave as if they have temporary crosslinks, called entanglements. The exact nature of the molecular mechanism of entanglements is still a subject of debate(ref.13), but the idea of molecules entangling with each other and forming interlocking loops, as illustrated in figure 11, provides a satisfactory picture of the situation which is consistent with observed behaviour. Entanglements are able to unwind and reform in response to changes in the local molecular environment. Hence entangled materials can undergo indefinite deformation, and so are fluids and not solids.

Because of the extended nature of the entanglement structures, relatively long times are required to produce changes in entanglement structure, so for short time scale deformations, entangled polymers behave like rubbers.
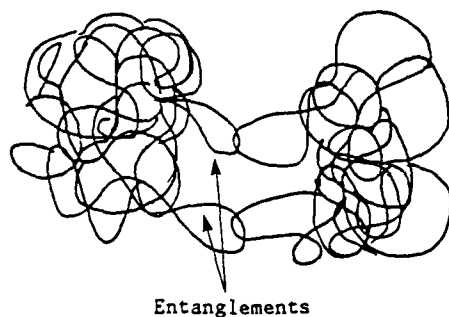
Entanglements

Figure 11. Schematic representation of molecules linked by entanglements

2.5.4   *Time dependence of elasticity*

So far the discussion has been in terms of an idealised elastic structure, where elastic deformation occurred without dissipation of energy. However, in real polymeric materials, segments of the molecular chain slide past each other during deformation, and viscous forces are involved in a similar way to low molecular weight materials. As discussed in Section 2.5.1, the viscosity of unentangled molecules can be written as

$$\eta = KNf_o,$$

where N is the number of segments, and f_o is the molecular friction factor for one segment. However, for entangled fluids, the number of segments, N, has to be increased to allow for the extra segments dragged along by the entanglements. Hence the viscosity can be written as

$$\eta = K'N^*f_o,$$

where N^* is calculated to take account of entanglements and K' is a constant similar to K. The effect of viscosity is to slow down or delay the response of the polymer to applied stress.

Materials which display a combination of viscous and elastic behaviour are known as visco-elastic materials.

The effect of interaction between elasticity and viscosity can be illustrated by considering the response of a rubber. If a rubber which has been held a for long time in a deformed state is released, it will tend to return to its equilibrium state. The return to equilibrium will not be immediate, however, because the motion will be resisted by the viscous forces between the molecular segments. The time to reach equilibrium will clearly be shorter for large values of the restoring force, which is proportional to G or E, and will be longer for high values of the viscous forces, or viscosity η. It is possible to define a time constant for the memory of the rubber, λ, as

$$\lambda = \eta/G \text{ in shear, and } \lambda = \eta T/E \text{ in extrusion.}$$

λ measures the timescale of the response of the material to deformations or stresses.

If a material is deformed at a rate which is high compared with the time constant, large stresses can be developed because there is insufficient time for viscous relaxation, and the apparent modulus is high. If the extension rate is lower than the time constant, the stresses are relatively low because the molecules relax by viscous flow, and the instantaneous modulus is low.

2.5.5   Elasticity in flow- Extensional Flow

In flowing from the large diameter of the extrusion press into the die, the fluid undergoes strong converging flow, which has a large extensional component, see Section 2.3 on Elongational Flow. The extensional stress decays at a rate related to the time constant of the fluid, and for long dies the stress is able to decay to an insignificant level by the time the material reaches the die exit. However for short dies the stress still has a significant value at the exit, and this residual stress causes the extrudate to swell on leaving the die.

2.5.6   *Elasticity in flow- shear flow*

The effects of elasticity are less obvious in shear, but they can be demonstrated by considering the situation illustrated in figu· 12. It can be seen that while the square ABCD undergoes shear, the diagonal AC is stretched to AC', so that in elastic materials an elastic force will be generated in that direction. Similar forces will be generated between all other points in the material. These forces can be resolved into two directions, along the direction of the flow, and perpendicular to it.
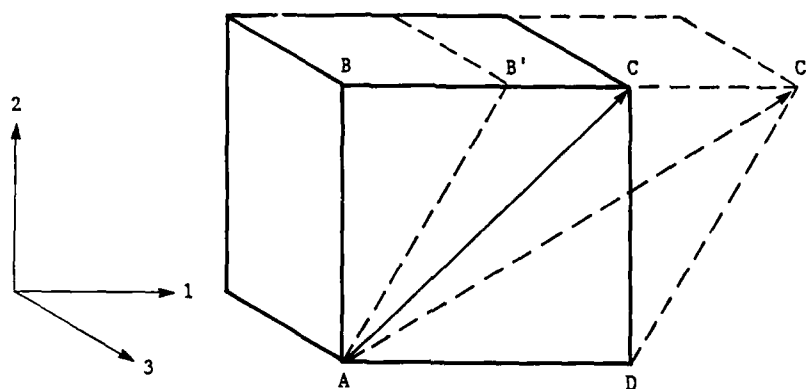
Figure 12. Elastic stretching in shear flow

Since the shearing takes place in 3 dimensional space, the stress and deformation should be described in terms of rank 3 tensors. However, to avoid the complication of having to use tensor analysis, we will illustrate the normal stress behaviour by making the simplification of replacing stresses by forces. A rigorous discussion in terms of tensors is given in many text books, including Tadmor and Gogos(ref.1).

The conventional coordinate system for describing viscometric flow is illustrated in figure 12.

The 1 direction is the flow direction.

The 2 direction is the direction along which velocity changes.

The 3 direction is the neutral direction.

The elastic force along AC' in figure 12 can be resolved into components in the 1 and 2 directions.

Forces which act along three mutually perpendicular directions, in this case the 1,2 and 3 directions, are known as normal forces. The simplest example of a set of normal forces is isotropic pressure, where the forces in the three directions are equal. Under isotropic pressure there is no net

force to cause deformation. It is only differences in the normal forces which have an effect on flow. There are 3 force differences between the 3 normal forces, but only 2 are independent. The 2 force differences which are conventionally used are known as the first and second normal force (stress) differences defined by

$$\text{First normal force difference} = N_1 = F_1 - F_2$$

$$\text{Second normal force difference} = N_2 = F_2 - F_3$$

In the case considered here, we have assumed that $F_3 = 0$. However, in physically realistic situations, it is usually the case that $N_2 \sim -0.2N_1$, so N_1 is the most important stress difference.

Specification of the viscosity, and the first and second normal stress differences, suffices to fully characterise the simple viscometric flow of an elastic fluid.

A spectacular demonstration of the effect of the normal elastic force generated in shear flow is the Weissenberg effect. If a rod is placed in a Newtonian fluid and rotated about its axis, as illustrated in figure 13, the level of the fluid adjacent to the rod drops as centrifugal force pushes the fluid away from the rod. However, if the Newtonian fluid is replaced by an elastic fluid, it is found that the fluid climbs up the rod as illustrated in figure 13. The explanation is that the shear flow around the rod generates an elastic normal hoop stress, squeezing the material inwards and upwards.

The most important effect of normal stresses in propellant processing is die swell from long dies. It has already been seen that elastic stresses generated in the extensional flow in the entry region of a die can cause swelling of a fluid as it exits from a short die. In a similar manner, the normal stresses generated by shear flow in long dies can also cause die swell. The normal stress in the flow direction in the die is equivalent to stretching, and while the fluid is being sheared in the die the stresses are maintained. However, when the constraints on the flow are removed as the fluid exits the die, the stresses relax by contracting the extrudate in the flow direction and expanding it in the radial direction. A theoretical expression which quantitatively relates die swell to the value of the first normal stress difference has been developed by Tanner(ref.14), viz:

$$D/D_0 = 0.1 + (1 + N_1/\tau_w)^2)^{1/6}$$

where D_0 is the capillary diameter, D is the extrudate diameter, and τ_w is the shear stress at the wall.

Newtonian Fluid   Elastic Fluid
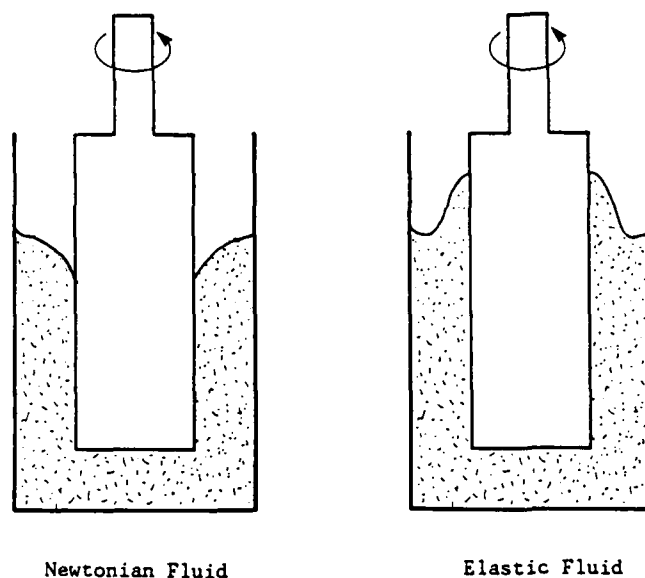
Figure 13. Difference between inelastic and elastic fluids in a rod stirring experiment

At higher shear rates and high levels of elasticity, flow instabilities occur. The general phenomenon of elastic flow instability has become known as melt fracture, even though true fracture does not usually occur. There appear to be several possible mechanisms, and melt fracture is far from being well understood. However, it is not productive to pursue this topic in relation to propellant processing, as melt fracture usually occurs at extrusion rates where the die swell would already be too large to be tolerated in production.

Normal stresses can also cause instabilities in rotary flow geometries, and these instabilities preclude the measurement of normal stresses above shear rates of about 1 s^{-1}.

2.6   Effect of fillers

The effects of fillers on flow are varied and complex, and there have been many studies of the effects in particular systems. There are several reviews of the subject, and one of the best is given by Vinogradov and Malkin(ref.2). We will consider the simplest case of a very dilute suspension initially, and then examine the effects of various complicating factors one at a time. For very dilute suspensions of spherical particles in a Newtonian fluid, Einstein derived the following expression for viscosity

$$\eta = \eta_s (1 + 2.5\varphi),$$

where η_s is the viscosity of the solvent or matrix, and φ is the volume fraction of filler. The particle size, or size distribution, has no effect on viscosity. This formula is of no practical use in propellant processing because it is restricted to vanishingly small concentrations.

The first level of complication is to allow the particle shape to become non-spherical, and to approximate the shape by an ellipsoid. At very low concentrations, where the hydrodynamic forces are unaffected by the presence of other particles, the viscosity increases from the spherical value as the shape becomes more ellipsoidal in both the prolate and oblate directions. The non-spherical shape gives rise to orientation effects which lead to the following effects; non-Newtonian viscosity, normal stresses, and differences in behaviour in shear and extension.

The first normal stress difference generally increases with increasing particle aspect ratio, but it may be decreased in cases where a yield stress occurs(ref.15). The development of non-Newtonian viscosity and normal stresses is a function of the filler properties only, and does not depend on the matrix being elastic.

In concentrated suspensions there are hydrodynamic interactions between the particles. There is no general theoretical analysis of this case, but a number of semi-empirical formulas can be used to fit experimental data. A useful measure of the concentration of a suspension is the ratio of the actual volume fraction of filler, φ, to the volume fraction at maximum packing density, φ^*. For equally sized spherical particles in hexagonal packing, $\varphi^* = 0.74$, while parallel packing of fibrous fillers gives $\varphi^* = 0.91$. For polydisperse systems the maximum φ^* is higher than mono-disperse systems. It is difficult to calculate φ^* in the general case.

A quantitative indication of how the low shear rate viscosity depends on φ/φ^* has been given by Bigg(ref.16), and is illustrated in figure 14.

At low concentrations of filler the matrix is a continuous phase and the filler is a discrete phase. However, as the concentration of filler is raised, a point is reached where the filler particles are forced into contact with each other, and a continuous filler phase is formed. At very high concentrations the particles may form strong contacts with neighbours leading to the formation of a rigid network in the material. A finite stress, the yield stress, must then be applied to cause flow. There is a tendency for smaller particles to produce higher values of the yield stress than larger particles. Particles smaller than about 1 μm show a strong tendency to agglomeration, which reduces φ^*, and hence increases the viscosity. Matrix material will also be rigidly bound in the interstices of the agglomerate, effectively reducing the matrix concentration. White et al measured yield stresses in extension, Ye, and in shear, Ys, and found Ye/Ys ~ 1.8, suggesting that a Von Mises criterion for plastic yielding applies for active fillers(ref.15).

Fibrous fillers with large length/diameter ratios can form stiff structures just through mechanical hindrance to the motion of the fibres by the random packing of other fibres: no chemical or physical bonds need be involved. The situation is similar to the entanglement of polymer molecules, as discussed in Section 2.5.3.
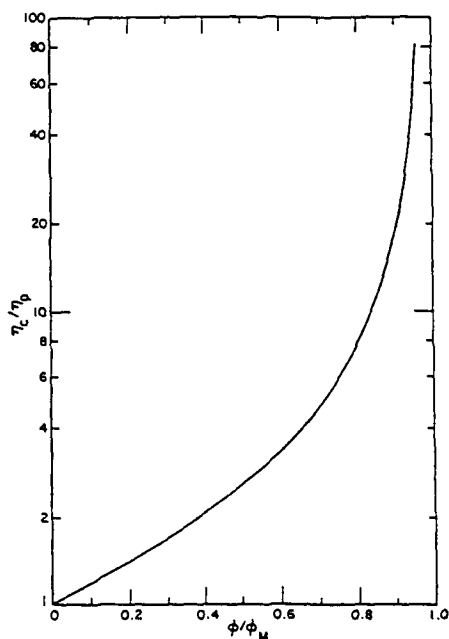
Figure 14.   Relative viscosity of a filled system as a function of the volume of filler relative to the
maximum packing fraction

Active, or reinforcing, fillers are those which have strong interactions either between the filler
and the matrix, or between the filler particles themselves. If the filler interacts with the matrix,
then there will be a layer of matrix molecules bound to the filler surface, and hence the particles
would be effectively enlarged, and concentration effects would be enhanced. A second type of
situation sometimes arises when the particles tie molecules together and act as crosslinks, greatly
increasing the modulus. Many carbon blacks are active fillers, and they bind to the matrix and
cause a considerable increase in modulus.

When the matrix is a viscoelastic medium, as opposed to a Newtonian fluid, the presence of rigid
fillers reduces elastic effects such as normal stresses and die swell. Non-reinforcing blacks reduce
the die swell of rubbers in proportion to their volume fraction, whereas reinforcing blacks reduce die
swell by a greater factor. The effects of reinforcing fillers are poorly understood.

The flow near the walls of a die or rheometer can show anomalous effects. There is a tendency for
the filler to migrate away from the wall and leave a matrix rich layer next to the wall. This layer
has a lower viscosity than the bulk material, and can give the appearance of slippage at the wall.
This effect is enhanced when the matrix is viscoelastic. The change in flow behaviour can usually
be quantified in the same manner as wall slip, see Section 2.2.2.

It is apparent that some rheological behaviour, such as non-Newtonian viscosity and normal stresses, can be caused by quite different fundamental mechanisms, and care must be used in ascribing particular mechanisms to observed behaviour. With the present state of knowledge it is only possible to list the general effects of fillers on flow as no comprehensive theory exists. In propellant processing it is necessary to determine the effect of each filler type in the various propellant matrices experimentally.

2.7   Viscous heating

2.7.1   General

The work done by the pressure on the fluid flowing down a capillary die causes a change in the internal energy of the fluid, which is manifested as an increase in temperature. The effects of this increase in temperature have been discussed at length (reference 4, chapter 5). If no conduction is assumed to take place in the fluid, then the temperature rise is given by

$$dT = \frac{-dP}{\rho Cv}$$

where dP is the pressure drop, ρ is the density, and Cv is the heat capacity at constant volume. If the thermal conductivity of the fluid is finite, but the die walls are well insulated, then the same formula gives the average temperature rise of the fluid. This temperature rise is usually of the order of a few degrees, and can often be neglected. However, the average temperature rise gives a misleading impression of the effect of viscous heating, as the heat is not generated uniformly throughout the die. The amount of heating is proportional to the product of the local shear stress and local shear rate. In the centre of the die this quantity is zero by symmetry, but it increases with radial distance to a maximum at the die wall. Hence the temperature rise near the die wall can be many times the average temperature rise.

Calculation of the effect of viscous heating is complicated by the fact that the viscosity is usually highly temperature dependent, and this dependence tends to reduce the overall rate of heat generation. Where the temperature is highest the viscosity is lowest, and so the flow rearranges to minimise the total energy of the system.

Calculation of the interaction between the temperature, viscosity, and velocity profiles is too complex to be undertaken analytically, and numerical methods are required. Both finite difference and finite element methods are used, but finite elements are more generally used because of the wider range of boundary shapes and conditions that can be easily incorporated.

The temperature and velocity profiles are strongly affected by the type of thermal boundary conditions at the die walls. If the walls are well insulated the appropriate boundary condition is adiabatic walls. In this case all the heat generated will be retained in the fluid and the temperature rise is greatest, with the maximum temperature rise occurring at the die walls. However, if the die walls are extremely efficiently cooled, then the appropriate boundary condition is isothermal walls. In this case much of the heat is carried away by the cooling fluid, and the temperature rise is minimised. For steady flow in long dies the maximum temperature occurs in the centre of the flow, and the fluid near the walls is at the wall temperature. Most practical cases are intermediate between adiabatic and isothermal walls, and the boundary condition can be approximated by assuming a constant heat transfer coefficient at the walls.

The amount of heating, and also the exit velocity profile, depend on the length of the die because for a given flow rate the pressure drop, and hence the amount of heat generated, increases with increasing die length. An additional factor is that longer dies allow more time for heat to flow towards the centre of the die, as well as to the walls.

In propellant processing the temperature rises can be very significant. Surface temperature rises of propellant flowing from a die with a length/diameter ratio of 50 have been measured as high as 30°C. An illustration of the effect of viscous heating in a typical die with different boundary conditions is given in figures 15 to 17. The die has a diameter of 2 mm and a length of 30 mm. A finite element program was used to calculate temperature profiles in the die for flow of a material with typical propellant rheological properties at average velocities of 100 mm/s and 25 mm/s. For a velocity of 100 mm/s the axial profile of maximum temperature is given in figure 15, and the radial profile at the exit is given in figure 16. $\beta = 0$ corresponds to a viscosity independent of temperature, together with adiabatic walls, and it can be seen that in this case the temperature rise is very large. The radial temperature profile for a velocity of 25 mm are given in figure 17. At this lower velocity there was greater time for the heat to flow to the centre of the die, and so the centreline temperatures are relatively higher.

2.7.2   *Effect of viscous heating on propellant processing*

The most obvious effect of viscous heating is an increase in throughput at a constant pressure, or equivalently, a drop in extrusion pressure at constant throughput. This effect can be beneficial when extruding very viscous doughs which may have to be extruded near the limit of the extruder capacity. However, several negative effects must be taken into account. The high surface temperature generated when heating is large can cause processing solvent to boil off, giving an irregular surface(ref.17). The stability of the propellant may also be affected if the temperature rise is too great.

In poorly gelatinised propellants the heating of the surface layer could change the degree of gelatinisation of the NC in that region. The change in gelatinisation may affect the rate of diffusion of deterrents into the propellant grains. Also, the temperature gradient in the radial direction would result in frozen-in stresses on cooling of the extrudate, which would increase the brittleness of propellant grains. The magnitude of these effects should be determined if viscous heating is significant.

2.7.3   Effect of viscous heating on die swell

Radial temperature gradients in fluids flowing in dies, particularly near the die exit, may cause large changes in the diameter of the extrudate. The temperature gradients can be caused not only by viscous heating, but also by maintaining the die at a different temperature from the bulk of the fluid.

For the case of an inelastic fluid, Tanner has developed a theory of the effect of temperature gradient on die swell(ref.18). He predicted large changes in swell for moderate changes in temperature gradient, and these predictions were confirmed by finite element calculations(ref.19).

Qualitatively, the effect can be explained in terms of the change in velocity profile caused by the temperature gradient. If the fluid near the die wall is hotter, it has a lower viscosity, so the velocity profile is steep near the wall, but more pluglike in the remainder of the fluid. When the fluid exits the die it has to undergo a smaller rearrangement in flow profile because of the pluglike flow in the die, and hence the die swell is less. On the other hand, if the fluid near the wall is cooler, the velocity profile would deviate in the opposite direction from plug flow, and the die swell would be increased.

For inelastic fluids, the inelastic heating effects are superimposed on the elastic behaviour, which is also affected by the temperature gradient. When the higher temperature is near the wall, the elastic modulus and the elastic time constant of the fluid are reduced. Since the effect of heating is greatest in the region where the elastic stresses are greatest, viscous heating significantly reduces die swell(ref.20).
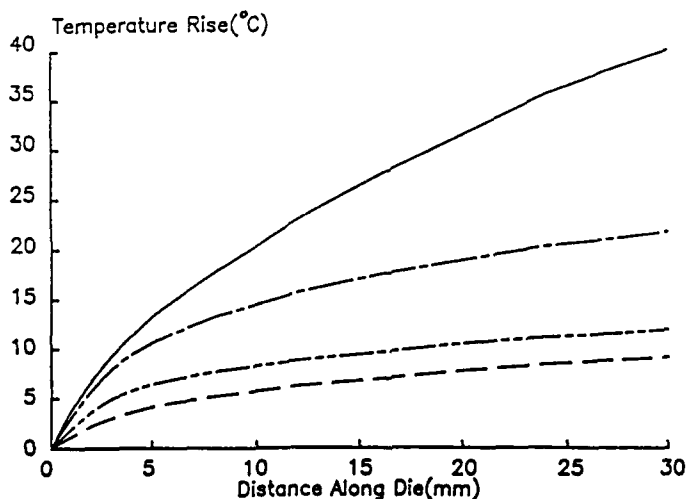
Figure 15.   Calculated axial profile of maximum temperature at an average velocity of 100 mm/s.
——— $\beta = 0$,— — — isothermal wall,— - —adiabatic wall,—----— constant heat transfer coefficient at the die wall
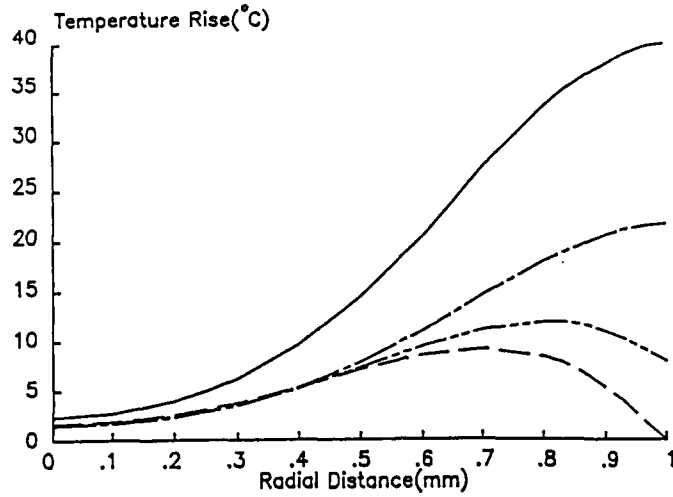
Figure 16. Calculated exit radial temperature profile at an average velocity of 100 mm/s.
————— β = 0,————isothermal wall,———— adiabatic wall,————— constant heat
transfer coefficient at the die wall
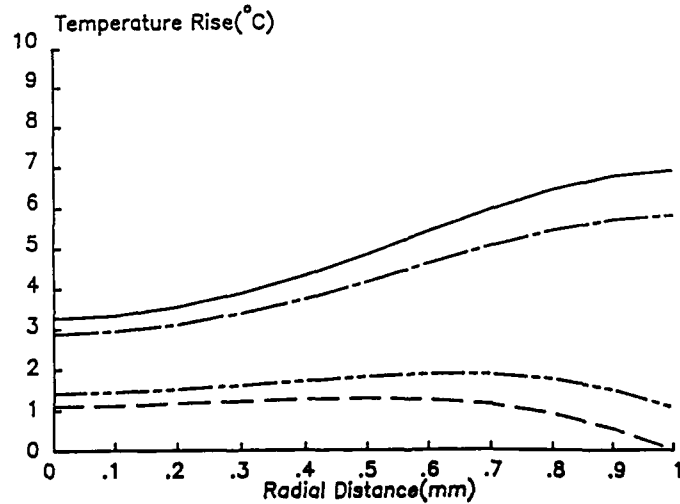
Figure 17. Calculated exit radial temperature profile at an average velocity of 25 mm/s.
————— b = 0,————isothermal wall,———— adiabatic wall,————— constant heat
transfer coefficient at the die wall

3. MIXING

3.1   General

The aim of propellant mixing is to produce dough which is homogeneous in both composition and temperature. It is also necessary to gelatinise the NC to the required level, and to break up any solid filler agglomerates and disperse the resulting particles.

We will start with a discussion of the current empirical descriptions of mixing, and then develop a fundamental description. Because the reader is likely to be most familiar with batch processing in propellant incorporators, the fundamentals of mixing will be discussed in that context first, and then developed further for other types of mixers.

3.2   Batch mixing

3.2.1   Mixing parameters

Mixing parameters tend to fall into two classes, controllable parameters, and measurable parameters.

Controllable parameters

(1)   Blade configuration

Mixers fitted with sigma blades are the norm in Australia, but mixers usually have double Naben blades in the UK. It is possible to change blade configuration, but this is not a routine operation.

(2)   Blade clearance

The minimum blade clearance is set by the manufacturer, but the blade tips are often ground down to increase the clearance. Ideally the clearance should be small to produce large shear stresses in the gap, but propellant manufacturers usually prefer large clearances because of concerns about safety.

(3)   Blade rotation speed

Altering blade speed is a simple method of affecting mixing behaviour, but it is not often used because the speed is fixed on many mixers. However, a variable speed drive can usually be added without too much difficulty.

(4)   Mix time

Currently one of the main parameters used to control the process is mix time. Unfortunately it has little fundamental significance when considered in isolation from other factors.

(5)   Mix temperature

The mixer jacket temperature is controlled by fluid circulation. Varying the temperature alters the viscosity of the dough, and hence the amount of work done in the mixer. The temperature would also affect the action of processing solvents on the NC, and so alter the gelatinisation.

Measurable parameters

(1)   Power consumption or torque

Power or torque can be used to measure the effect of small changes in the mixing process, such as temperature or blade speed. It is theoretically possible to relate torque or power to viscosity and mixing efficiency by either experimental calibration or calculation.

(2)   Tracer dyes

The only direct way to follow flow patterns in a mixer is by using tracer dyes or different coloured doughs. There have been a number of informative flow visualisation studies made in small internal rubber mixers of the Banbury type using these techniques.

(3)   Mix temperature

For a fixed amount of external heating or cooling, the dough temperature gives indication of work input and dough viscosity.

3.2.2   Scale up of processing equipment

Studies of processing parameters are usually carried out at the laboratory or pilot scale, and the question of scaling up to production size becomes important. An engineering approach to scaling up is to choose dimensionless variables to describe the process. If these variables are indeed appropriate, then keeping them constant on scaling up should ensure that the process remains the same. Various dimensionless numbers are used to relate the sizes of mixers, temperature effects, and elastic effects. Often it is not physically possible to maintain all numbers constant during scale up, e.g. heat generation increases as the cube of the size, while heat loss increases as the square of the size.

Some of the scale up procedures which have been suggested in the literature are listed below (reference 21, page 612). Various combinations are used in practice.

(a)   All linear dimensions and rotation frequency scaled up proportionately.

(b)   Constant maximum shear stress.

(c)   Constant mixing time.

(d)   Constant dough temperature.

(e)   Constant blade clearance, with rotation speed reduced in inverse proportion to blade radius.

(f)   Total shear strain (TSS)

TSS is a dimensionless number, designated Γ, which is defined by

$$\Gamma = \text{shear rate.time.volumetric throughput.land-length ratio}$$

where volumetric throughput is the theoretical fraction of the volume of the material which is sheared in each revolution of the blades, and the land-length ratio is the blade tip width divided by the circumference of the mixing troughs. Royal Ordnance have used the TSS as a basis for empirical scale up factors(ref.22).

(g)   Work Unit, introduced by Van Buskirk(ref.23), W_u, is given by

$$W_u = W_t/V_b = \int_{t1}^{t2} P(t).dt/V_b$$

where W_t is the total work done in the mix cycle, V_b is the volume of the dough, and $P(t)$ is the power consumption at time t. Van Buskirk obtained good correlation of various properties of carbon black filled rubbers, which were mixed under different conditions, but with equivalent values of W_u.

3.2.3   Rubber mixing

The parameters considered above do not give fundamental information about the state of the material in the mixer, as they treat the mixer as a black box, and it is not always clear which factors are appropriate to apply in a particular case. It would be of great benefit if a comprehensive model of the mixing process could be developed. No such model exists at present, but a fruitful method of approach has been to break the mixing process into its elements and then study each separately. This procedure allows optimisation of each part of the process, even if all the parts cannot be joined together in a coherent manner.

A large amount of work has been done in the rubber industry on modelling parts of the mixing cycle, and some of the results can be applied to propellant mixing.
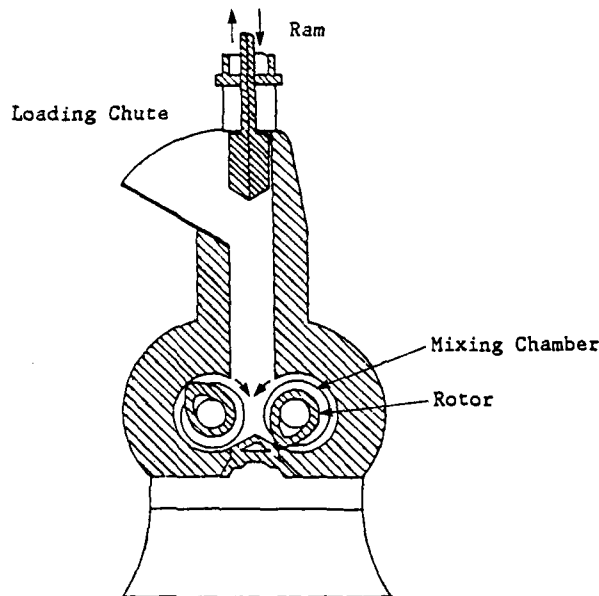
Figure 18. Schematic representation of a Banbury type of internal mixer

Rubber mixing is often carried out in internal mixers which are capable of producing high shear stresses. A typical Banbury mixer is illustrated in figure 18. The ingredients are loaded into the loading chute and the ram is used to compact them into the mixing chamber. The rotors turn at slightly different speeds, which causes the material to continually flow from one side of the chamber into the other. The rubber undergoes elongation and shear flow near the blade tips, which produces large stresses. The rest of the volume of the chamber allows low shear mixing of the rubber. The fraction of the chamber which is occupied, known as the fill factor, is usually in the range 0.7 to 0.8.

One of the main reasons for mixing rubbers is to incorporate carbon black into the rubber matrix. Typically 30% carbon black is added. Initially the carbon black is in the form of agglomerates which often enclose a relatively large amount of free space. The mixing process consists of breaking up these agglomerates into their fundamental units, and then distributing them uniformly throughout the rubber.

A similar process of particle breakup occurs in mixing the rubber itself. Nakajima described the mixing of powdered rubber which has an average particle size of about 250 μm(ref.24). After the mixing cycle the size is reduced to about 0.1 μm, which allows good intermixing of the rubber with the carbon black.

Two types of mixing are assumed to occur during this process; dispersive or intensive mixing, and distributive or extensive mixing.

Dispersive mixing increases the interfacial area of the components of the mixture. In rubber processing, the increase in area is achieved by breaking up the carbon black agglomerates. More generally, if one (or more) of the components has a yield stress for either flow or rupture, then the amount of breakup of that component will be determined by the extent to which the local value of the hydrodynamic stress exceeds the yield stress. Hence the local value of stress is the important parameter.

Distributive mixing involves the uniform distribution throughout the material of the dispersed components which were produced by intensive mixing. Distributive mixing also occurs when the components are liquids without a yield stress. Strain is the important variable, and rate of strain or stress do not affect the degree of mixing, although the stress will affect the power requirements.

3.2.4   NC Propellant mixing

The NC initially consists of fibres, which have structure made up from fibrils and molecules, see figure 19. Fibrils are about 25 μm in diameter, and are made up of ordered bundles of microfibrils which are about 3 μm in diameter.

It is the purpose of mixing to break down most of the fibres into fibrils and molecules, which then form a matrix phase to bind the remaining fibres and fibre fragments into a cohesive whole. A discussion of the processes occurring in mixing NC propellants has been given by Ayerst(ref.25), but the emphasis was on casting powders for cast double base propellants, and the approach was slightly different from the approach used here.

In the solvent mixing process, the structure of the NC fibres is weakened by the addition of solvents. The solvents have two effects; they totally dissolve some of the fibres into their constituent molecules, and they penetrate other fibres and weaken the interfibrilar and intermolecular bonds. When the weakened fibres pass through the high stress regions in the mixer, the fibres are broken down into fragments ranging in size from bundles of fibrils to molecules. These fragments are then be distributed throughout the mixture, thereby increasing the proportion of the matrix phase. When sufficient matrix phase is formed for the mixture to bind up into a coherent dough, the mixture is said to have "bound-up", or "doughed-up". Further mixing reduces the fibre content, and breaks up the larger fibre fragments into smaller fragments.

Once a dough is formed, the stresses are more efficiently transmitted between components of the mixture, and the torque required to operate the mixer rises. Dough-up is often accompanied by an increase in temperature, because of the extra energy input required to overcome the higher torque.

LUMEN

S_3

S_2
20°-30°

REVERSAL→

S_1 — Thin lines represent fibrils
20°-35°

PRIMARY
WALL
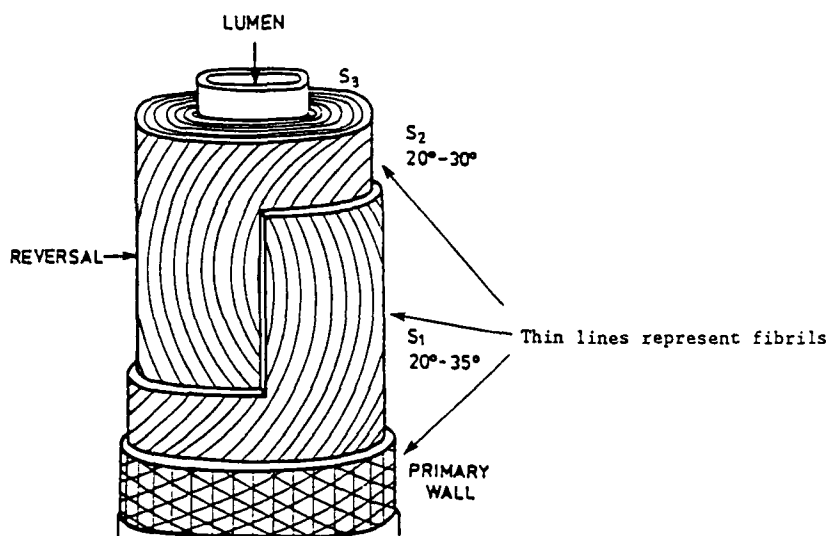
Figure 19. Structure of a cotton NC fibre

The process of breaking down the fibres into fibrils and molecules is generally known as gelatinisation, and the degree to which the process has occurred is known as the degree of gelatinisation. To give a totally accurate description of the state of gelatinisation of a dough or propellant, it would be necessary to quantify the relative fractions of the amount of each structural element. Gelatinisation is perhaps an unfortunate term to apply to NC because the word gel usually signifies a network structure in the material, and a gel does not necessarily form in NC doughs.

Before dough-up, the mixture resembles the inelastic material which was discussed in Section 2.4.2, and illustrated in figure 10. The particles in the mixture tend to be rigid, and only weakly adhere to each other. On the other hand, if gelatinisation were to be carried to completion, the material would consist of entangled molecules, similar to the elastic material in figure 10. Such a material would be difficult to mix, as it would strongly resist the deformation required for it to undergo to pass through the gap between the blade and the wall. A more worrying consequence, however, would occur when the dough was extruded, because the dough would swell greatly on exiting the die, or else suffer melt fracture. Hence the aim of mixing unfilled propellants is to only partially gelatinise the NC, and leave a large proportion of the fibres and fibrils to stiffen the dough and diminish the elastic behaviour. Determining the mixing time which produces optimum gelatinisation is a major problem for propellant processors, and is the biggest factor in determining scale-up factors.

In filled propellant compositions, the requirement to retain a proportion of fibres does not apply, as the fillers perform the function of stiffening the dough. The aim with filled propellants is to almost fully gelatinise the matrix and cause it to totally wet the filler particles. Achieving dough-up in a short time is a major requirement, and predicting dough up time for scaling up is very difficult.

The analogy between NC propellant mixing and rubber mixing is quite apparent. Dispersive mixing breaks down NC fibres and fibrils in propellants in a similar manner to the break down of carbon black agglomerates and rubber particles in rubber mixing. The fibre fragments are then uniformly distributed throughout the dough in the low shear regions of the mixer, analogously to distribution of carbon black agglomerate fragments in distributive mixing in a rubber mixer.

3.2.5   Model of the mixing process

A model of the mixing process in rubber processing has been developed by Manas-Zloczower and Tadmor, and their co-authors(ref.21,26), in a series of papers. A slightly different analysis has been given by Nakajima(ref.9,24). With suitable modifications this model is applicable to NC propellant processing. The overall flow pattern in the mixer is modelled as a well mixed region between the rotors from which a continuous stream of material is forced through the high stress region near the blade tip. Hence the distributive and dispersive types of mixing are explicitly associated with separate parts of the mixer. A schematic representation of the mixing process is given in figure 20.

The distributive mixing process in internal rubber mixers has been studied with great success using flow visualisation techniques. The effect of variables such as fill factor, rotor speed and temperature have been readily determined from observing the development of flow patterns of coloured doughs. Such techniques should be equally applicable to studying distributive mixing of propellant doughs.
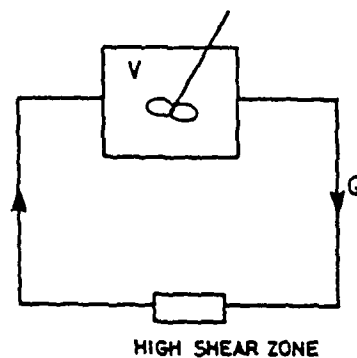

HIGH SHEAR ZONE

Figure 20.   Schematic representation of an internal mixer. V represents the well mixed region between the rotors, and Q is the flow in the high shear rate regions on the mixer

Dispersive mixing is much more difficult to study, because quantifying dispersion involves both the determination of the flow field in the high stress region to allow calculation of the local stresses, and also the determination of the response of the agglomerates or fibres to stress.

Agglomerate or fibre rupture occurs when the hydrodynamic stresses exceed the cohesive strength. There are various calculations in the literature on the mechanism of particle breakup and the effect on the flow field. Aggregates tend to break in halves, but fibres may not do this because the weakest parts of the fibres may be randomly distributed along the length of the fibres. However, it may be reasonable to assume that on average the fibres and fibre fragments will break in halves. The region ahead of the blade is as important as the gap region, because the converging flow there has a large extensional component, which is more effective in dispersion than is shear flow (reference 21, page 599). A model predicts that dispersion forces are twice as high in elongational flow than in shear flow for the same deformation rate (reference 21, page 609), but high continuous shear is easier to obtain.

A particularly promising method of quantifying dispersive mixing, which also provides a scale-up parameter, has been described in a separate paper by Manas-Zloczower and Tadmor(ref.27). A quantity designated Xt^* is defined, where X is the fraction of agglomerates broken in one pass through the gap, and t^* is a dimensionless time given by $t^* = t/t'$, where t is the actual mix time, and t' is the mean residence time in the high stress region.

Using the Xt^* parameter, the volume fraction of undispersed agglomerates as a function of time, designated by ψ, is given by

$$\psi = 1 - \Gamma(n+1, Xt^*),$$

where Γ is the incomplete Gamma function, and n is effectively the number of times the agglomerates must be broken in half to reduce them to their fundamental units, and is given exactly by

$$Vo/2^{(n+1)} < Vcr < Vo/2^n,$$

where Vo is the initial agglomerate volume, and Vcr is the volume of the fundamental unit. n is a function of the structure of the carbon black (or NC fibre) only, because it depends on the way the structure is broken up, and so it is fixed for a given material. Hence ψ depends only on Xt^*.

The value of X, the fraction of agglomerates broken in one pass through the high stress region, is calculated from the blade dimensions, the local values of the stress, and the structural parameters of the agglomerate. The value of t' is calculated from the flow profile near the blade tip. Manas-Zloczower and Tadmor provide formulae for calculating the various parameters, and using these they obtained reasonable agreement with experimental results from rubber mixing(ref.27).

To produce a more exact description of the local stress field than that provided by
Manas-Zloczower and Tadmor, it is necessary to analyse the flow near the blade tip in detail. In
particular, it is necessary to determine what fraction of material goes past the blade tip and is
highly sheared, and what fraction recirculates in the low shear region.

The higher the stresses in the gap region, the greater will be the pressure in the region before the
gap, and the less the amount of material which will be dragged through the gap.

The flow in the region of the blade tip, in either rubber mixers or propellant mixers, is illustrated in
figure 21. There are three main flows involved; flow through the gap, ML, flow in the
circumfrential direction, MR, and flow along the blade almost parallel to the mixer axis, MA. The
flow at the blade tip was accurately determined for a wide range of mixing conditions in a small
rubber mixer by Freakley and Patel(ref.28,29). They mounted 20 pressure transducers in the walls of
the mixer in a grid pattern, see figure 22. The pressure from each transducer was monitored as a
function of time. From a detailed analysis of the pressure traces, plus a knowledge of the rheology
of the rubber obtained by separate measurements, profiles of shear rate, velocity and stress were
calculated for the region around the blade tip. Freakley and Patel found that the amount of
material flowing through the gap, and the stress profile in the gap, was strongly affected by blade
speed, fill factor and temperature.

The methods used by Freakley and Patel could readily be applied to the study of propellant mixing
by suitably instrumenting a small mixer. The flow calculations could be improved over those of
Freakley and Patel by using finite element analyses, based on computer programs available at
WSRL. Hence it should be possible to monitor the stress and strain history of propellant doughs,
and obtain empirical correlations with the degree of gelatinisation so produced.
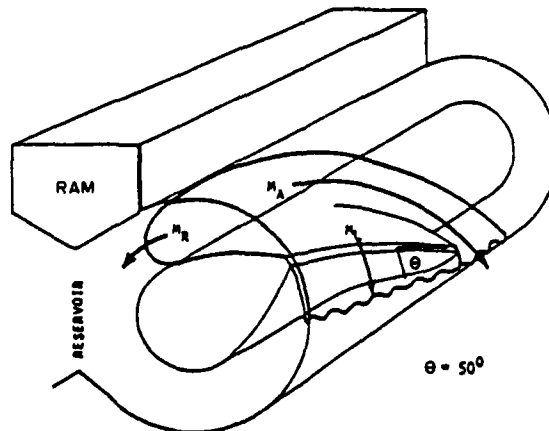

Figure 21.   A simplified layout of the dispersive mixing region of an internal mixer showing the
              components of material flow
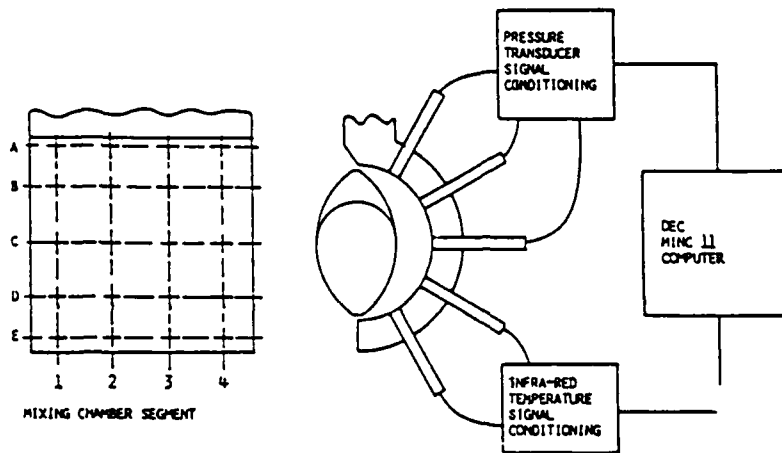
Figure 22. Schematic layout of the mixer monitoring system

3.3   Screw Mix-Extrusion

3.3.1   General

In this section we will review some of the current knowledge about the processes occurring in SMEs. Detailed descriptions of the machines will not be given, as there is a wealth of information available from the manufacturers on this subject. The discussion will be confined to Werner-Pfleiderer ZSK machines with two flighted screws. Fong has reviewed attempts to produce propellants by SME up to 1986(ref.30). It appears that while single and double base propellants can be made, there may still be scope for optimising their manufacture. However, there appear to be real problems in the processing of triple base propellants.

SME is fundamentally different from batch processing. In batch processes, dispersive mixing alternates with distributive mixing continuously, and the operator carries on the process until the desired degree of dispersion is obtained. In SME, some distributive mixing occurs by the action of the conveying screws in the feed zone which tends to distribute feed materials uniformly. Dispersive mixing occurs in a high stress zone made up of kneading blocks or reverse pitch screws. This zone is followed by a distributive mixing zone of conveying screws to distribute all the fragments generated in the dispersing zone, and also to build up pressure for extrusion.

The conveying screws are very efficient distributive mixers because of the geometry of the flow in the intermeshing region. Mixing is most efficient when the shear occurs perpendicularly to the local orientation in the material. This situation occurs each time the material passes through the intermeshing region, as illustrated in figure 23. The flow in the first chamber is tangential to the

first flight, but it undergoes a right angle change in the second chamber to be tangential to the second flight. While this geometry is very good for distributive mixing, it is not so good for dispersive mixing, and therefore kneading blocks and reverse direction screws are required.
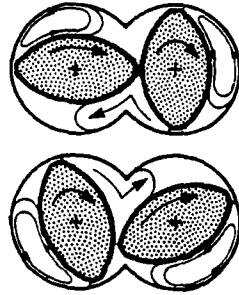
Figure 23. Change in flow direction in the intermeshing region of a twin screw extruder

In the batch process the mixing can continue until the desired concentration of dispersed particles in the dough is reached. However, in SME the space along the length of the machine for dispersive mixing is preset, and hence is not a process control variable. Control of the process has to be effected by varying temperature, rotation speed, and fill factor.

It is not worthwhile in this paper giving detailed reviews of models of flow in SMEs because the current models are too simplified. They usually assume no leakage flow, neither past the flight tips or back through the intermeshing region, and also the viscosity is assumed to be Newtonian. We will be concerned mainly in this paper with practical descriptions of flow in SMEs, and in developing semi-empirical parameters to quantify the process. This lack of fundamental design principles has forced the building block principle of screw design on manufacturers.

3.3.2   *Parameters important in screw mix-extruders*

Controllable parameters

(1)   Screw configuration.

(2)   Screw rotation rate.

(3)   Feed rate or fill factor.

(4)   Axial temperature profile of the barrel.

(5)   Die geometry and number.

Measurable parameters

(1)   Strain Distribution Function (SDF)

This parameter provides the best description of the strain history in the mixer. However, because there is at present no quantitative description of the complete flow through a machine, it is not possible to calculate the SDF exactly(ref.1). It is mainly of academic interest, but it will be useful in future when better models of flow are developed. The SDF is a more sophisticated version of the total shear strain(TSS) concept used to describe batch mixing (Section 3.2.2).

(2)   Specific Energy Consumption (SEC)

The SEC has been defined by Rauwendall as the rate of energy input per unit throughput(ref.31). The SEC is essentially the same as the work unit, Wu, used in batch mixing, and it gives a measure of the total deformation of the material.

$$SEC \sim \tau.\dot{\gamma},$$

where τ' is an average stress, and $\dot{\gamma}'$ is an average strain.

(3)   Residence Time Distribution (RTD)

This is a particularly important parameter for continuous processing, and its use in twin screw extrusion is discussed by Rauwendaal(ref.31). A narrow distribution is desirable for product uniformity, and for explosives it is also necessary to have short maximum residence times to avoid degradation and possible ignition of the dough. The RTD is determined by the velocity profile throughout the machine. However, the velocity profile cannot be calculated with sufficient accuracy at present, so the RTD must be measured experimentally.

One method of measuring the RTD is to inject a pulse of a tracer material into the feed section of the machine, and monitor the concentration of the tracer as it exits the machine. The resulting residence time distribution is known as the external RTD, or the age distribution of the material, f(t). f(t) is defined by

$$f(t) = C(t) / \int_{0}^{\infty} C(t') \, dt'$$

where C(t') is the concentration of the tracer leaving the machine at time t'.

The cumulative external distribution function F(t) is defined by

$$F(t) = \int_0^t C(t')\,dt' \Big/ \int_0^\infty C(t')\,dt'$$

f(t) and F(t) are illustrated in figure 24.
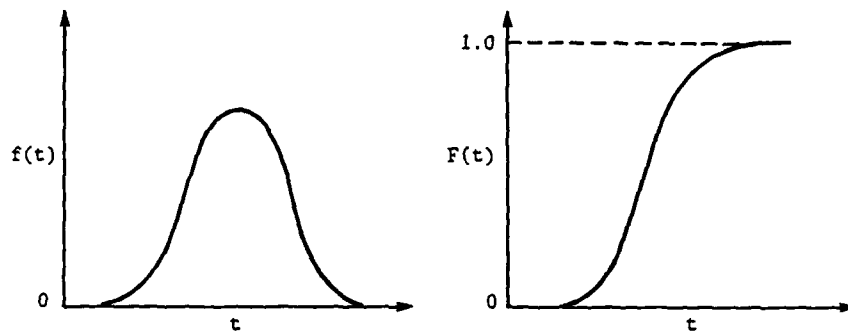
Figure 24. External residence time distributions

A second type of RTD known as the internal age distribution function, g(t), has also been used(ref.31). g(t) measures the fraction of the material remaining in the machine after time t. This distribution, when plotted as log(g(t)), has the advantage of accentuating the long time tail, as illustrated in figure 25. The relationships between f(t), g(t), and F(t) are given in Tadmor and Gogos(ref.1).
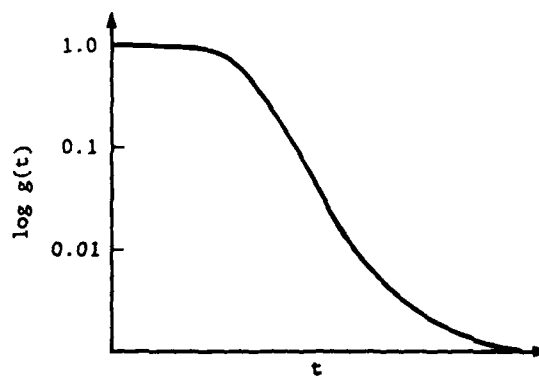
Figure 25. Internal age distribution

A further important parameter is the average residence time, t*, given by

$$t^* = \int_0^\infty t.C(t)\, dt \Big/ \int_0^\infty C(t)\, dt,$$

or more simply,

$$t^* = \frac{\text{filled volume}}{\text{volumetric throughput}}$$

In corotating extruders the RTD has a tail at long times, and the magnitude of this tail can be important for materials like explosives which are heat and shear sensitive. It is important that the RTD be measured under conditions where the tail is not lost(ref.32). The tail can be quantified by the concept of hold back, defined as the difference in area under the cumulative age distribution curves for pure plug flow, and the actual measured cumulative age distribution(ref.31).

Many different types of tracer have been used to measure RTD, but the easiest to use is neutron activated MnO_2(ref.33). This material has a half life of $2\frac{1}{2}$ hours, and so extruded material containing it is safe to handle after about 24 hours. MnO_2 has the advantage over other types of tracer that it can be detected by radiation counters at any position along the extruder barrel, so the effect of the various screw sections can be determined simultaneously. Most other tracers can only be detected in the material as it exits the extruder.

3.3.3   Effect of processing variables on measurable parameters

The effects of controllable (ie operating) parameters on the RTD and SEC were studied by Kao and Allison(ref.34). At low throughputs the SEC and average residence time, t*, increased sharply, and the RTD widened. Increasing the screw speed by a factor of three for a constant throughput reduced t* by about 30%, but under these conditions the leakage flows past the flight tips and the intermeshing zone had a large effect. On the other hand, high throughputs at low screw speeds reduced leak flows, t*, and the SEC, and also narrowed the RTD.

Kao and Allison compared the performance of two types of screw, one with only conveying elements, and another with four kneading elements interspersed between conveying elements. The average residence time was 50% longer with the screw with the kneading elements, but the RTD was nearer to that of plug flow. The barrel axial temperature profile had no effect on the RTD.

Rauwendaal studied the differences between counterrotating and corotating machines on the extrusion of high density polyethylene(ref.31). The machines were a Werner-Pfleiderer ZSK28

and a Leistritz counterrotating machine. The main difference in the types of machine was that the corotating unit has considerable opportunity for material to leak back to the previous thread on the other screw, and the counterrotating was a better dispersive mixer.

3.3.4   Extrusion pressure development

In order to develop the pressure required for extrusion, the screws in the region before the die must be fully filled. The flow in this region is complicated, because the extrusion pressure causes backflow, since the screw channels are effectively open in the corotating geometry. The amount of backflow affects the overall throughput, and a method of predicting throughput as a function of pressure is required.

An analysis of pressure gradient vs throughput in a 3 flighted SME has been undertaken by Denson and Hwang(ref.35). They made some fairly limiting assumptions including; (1) The viscosity is Newtonian, (2) For analysis purposes the flow channels can be unwound with the barrel wall becoming flat, (3) The flow in any channel does not affect the flow in any other channel, (4) The flow is isothermal.

Solution of the equations of motion by finite element methods produced curves of throughput vs pressure gradient for a number of screw geometries. Once the pressure gradient for a given throughput has been determined, the length of screw required to build up the extrusion pressure is easily calculated. Writing the throughput and pressure gradient in dimensionless forms leads to a relationship between them which is independent of the following factors; screw diameter and length, rotational speed, and the viscosity of the material. Hence this analysis could be used to define conditions for scaling up.

Unfortunately for propellant processors, the viscosity of propellant materials is far from Newtonian, as values of the power law exponent can be as low as 0.2, and hence the Denson and Hwang analysis cannot be applied directly. However, their equations could be solved for conditions appropriate for propellant processing using a suitable finite element program.

3.3.5   Devolatilisation

In the case of extrusion the screw channels had to be fully filled. However, for devolatilisation the screws are only partly filled to allow the generation of free surfaces to allow the volatile species to evaporate. A model of the devolatilisation process has been developed by Secor(ref.36). The model relates the ratio of entrance to exit concentrations of the volatile species to the dimensions of the screws, the rotation speed, the throughput and the diffusion coefficient.

Since the screw channels are only partly filled, the material piles up against the leading edge of the flights, and is carried along in a more or less uniform layer on the face of the flights. In the intermeshing region between the screws the material undergoes a large amount of distributive mixing. Secor models this flow in a manner illustrated in figure 26. The curved paths correspond to exposure of a surface of material of a uniform depth on the face of the flight, which occurs in a

series of intervals. The straight paths correspond to perfect mixing which occurs in a time very short compared to the exposure time. A further assumption is that the diffusion coefficient is constant.

The rate of diffusion from one flight is given by

$$AeCo(4Do/\pi t)^{1/2}$$

where Ae is the exposed surface area, Co is the initial concentration of the volatile species, Do is the diffusion coefficient and t is the exposure time. By calculating the available area of the screw faces, and making several approximations, Secor derived the following expression for the ratio of the initial concentration to the final concentration, Cn, after n exposures.

$$\frac{Co}{Cn} = \exp\left\{\frac{nA}{Q}\left(4\,Do\,f\,\frac{N}{\pi}\right)^{\frac{1}{2}}\right\} = \exp\left\{n\frac{A}{Q}\left(4\,Do\,f\,\frac{N}{\pi}\right)^{\frac{1}{2}}\right\}$$

where Q is the volumetric throughput, f is the fraction of the flight surface that is exposed, and N is the rotation speed.
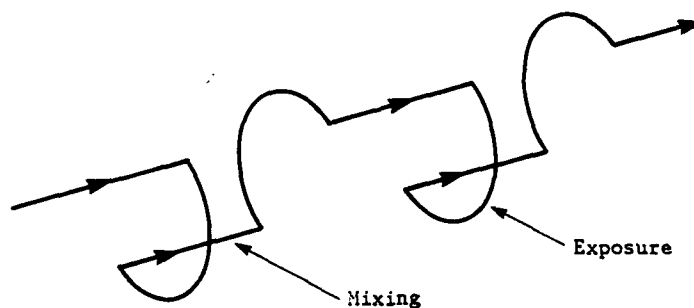
Figure 26. Idealised flow in the devolatilising region

An experimental test of the model was done using a specially made single flight extruder. The rate of desorption of a Freon dissolved in a polybutylene was measured. The calculated and observed desorption agreed within 15%. However, it would be expected that the accuracy in predicting the desorption on commercial machines would be less. In commercial machines the rate of removal of the desorbed gas may be less than ideal. Also the geometry of twin flighted screws would be more complicated than the single flighted screw used by Secor. Allowing for the limitations of the model, it appears to give a reasonable method of estimating the performance of devolatilising screws, and may aid in determining scale-up factors.

REFERENCES

No.	Author	Title
1	Tadmor, Z. and Gogos, C.G.	"Principles of Polymer Processing". John Wiley, New York, 1979
2	Vinogradov, G.V. and Malkin, A.Ya.	"Rheology of Polymers". Mir Publishers, Moscow and Springer-Verlag, Berlin, 1980
3	Bird, R.B., Armstrong, R.C. and Hassager, O.	"Dynamics of Polymeric Liquids, Vol 1". John Wiley, New York, 1977
4	Collyer, A.A. and Clegg, D. W.	"Rheological Measurement". Elsevier Applied Science, London, 1988
5	Tanner, R.I.	"Engineering Rheology". Clarendon Press, Oxford, 1985
6	Han, C. D.	"Rheology in Polymer Processing". Academic Press, New York, 1976
7	Leblanc, J.L.	"Factors Affecting The Extrudate Swell and Melt Fracture Phenomena of Rubber Compounds". Rubber Chemistry and Technology, 54, 905, 1981
8	Warren, R.C.	"The Effect of Liquid Crystal Structure on the Rheological Properties of Nitrocellulose-Dimethylacetamide Solutions". Rheol. Acta. 23,544, 1984
9	Nakajima, N.	"Energy Measures of Efficient Mixing". Rubber Chem. Tech., 55, 931, 1982
10	Warren, R.C. and Starks, A.T.	"Multiple Flow Regimes in the Extrusion of Nitrocellulose Based Propellant Doughs". WSRL Technical Report, WSRL-TR-43/88
11	Cogswell, F.N.	"Converging Flow of Polymer Melts in Extrusion Dies". Polym. Eng. Sci., 12, 64, 1972

12   Bueche, F.   "Physical Properties of Polymers".
                                            Interscience Publishers, New York, 1962

13   Graessley, W.W.   "The Entanglement Concept in Polymer Rheology".
                                            Advances in Polymer Science, Vol.16, Springer-Verlag,
                                            Berlin, 1974

14   Tanner, R.I.   "A Theory of Die Swell".
                                            J. Polym. Sci., A2, 8, 2067, 1970

15   White, J.L.,   "Experimental Studies of the Influence of Particle and
        Czarneck, L. and   Fibre Reinforcement on the Rheological Properties of
        Tanaka, H.   Polymer Melts".
                                            Rubber Chem. Tech., 53, 823, 1980

16   Bigg, D.M.   "Rheological Behaviour of Highly Filled Polymer
                                            Melts".
                                            Polym. Eng. Sci., 23, 206, 1983

17   Baker, F.S. and   "The Development of Modern Gun Propellants as a
        Carter, R.E.   Function of Basic Research".
                                            Proceedings ADPA Conference, Picatinny, NJ, USA, 1984

18   Tanner, R.I.   "A New Inelastic Theory of Extrudate Swell".
                                            J. Non-Newt. Fluid Mech., 6, 289, 1980

19   Phouc, H.B. and   "Thermally Induced Extrudate Swell".
        Tanner, R.I.   J. Fluid Mech., 98, 253, 1980

20   Carter, R.E. and   "Extrusion Stresses, Die Swell, and Viscous Heating
        Warren, R.C.   Effects in Double Base Propellants".
                                            J. Rheol. 31, 151, 1987

21   Manas-Zloczower, A.,   "Dispersive Mixing in Rubber and Plastics".
        Nir, A. and   Rubber Chem. and Tech., 57, 583, 1984
        Tadmor, Z.

22   Arber, A.W.   "An Empirical Design Guide for Incorporators used in
                                            Solvent Propellant Processing".
                                            ROF Memorandum No.2

23   Van Buskirk, P.R.,   "Practical Parameters for Mixing".
        Turetzky, S.B. and   Rubber Chem. Tech. 48, 577, 1975
        Gunberg, P.F.

24   Nakajima, N.   "An Approach to the Modeling of Mixing of Elastomers".
                                                Rubber Chem. Tech. 54, 266, 1981

25   Ayerst, R.P.   "Some Observations on the Incorporation Stage in
                                                Colloidal Propellant Processing".
                                                Available in manuscript

26   Manas-Zloczower, A.,   "Dispersive Mixing in Internal Mixers- A Theoretical
        Nir, A. and   Model Based On Agglomerate Rupture".
        Tadmor, Z.   Rubber Chem. and Tech., 55, 1250, 1982

27   Manas-Zloczower, I. and   "Scale-up of Internal Mixers".
        Tadmor, Z.   Rubber Chem. and Tech., 57, 48, 1984

28   Freakley, P.K. and   "Internal Mixing: A Practical Investigation of the Flow
        Patel, S.R.   and Temperature Profiles during a Mixing Cycle".
                                                Rubber Chem. Tech. 58, 751, 1985

29   Freakley, P.K. and   "Internal Mixing: A Practical Investigation of the
        Patel, S.R.   Influence of Intermeshing Rotor Configuration and
                                                Operating Variables on Mixing Characteristics and Flow
                                                Dynamics".
                                                Polym.Eng. Sci., 27, 1358, 1987

30   Fong, C.W.   "Manufacture of Propellants and Polymer Bonded
                                                Explosives by Screw Extruders".
                                                WSRL Technical Report, WSRL-0456-TR

31   Rauwendaal, C.J.   "Analysis and Experimental Evaluation of Twin Screw
                                                Extruders".
                                                Polym. Eng. Sci., 21, 1092, 1981

32   Todd, D.B.   "Residence Time Distribution in Twin-Screw Extruders".
                                                Polym. Eng. Sci., 15, 437, 1975

33   Wolf, D.,   "Residence Time Distribution in a Commercial
        Holin, N. and   Twin-Screw Extruder".
        White, D.H.   Polym. Eng. Sci., 26, 640, 1986

34   Kao, S.V. and   "Residence Time Distribution in a Twin-Screw Extruder".
        Allison, G.R.   Polym. Eng. Sci., 24, 645, 1984

35   Denson, C.D. and   "The Influence of the Axial Pressure Gradient on Flow
      Hwang, B.K.   Rate for Newtonian Liquids in a Self Wiping,
                              Co-Rotating Twin Screw Extruder".
                              Polym. Eng. Sci., 20, 965, 1980

36   Secor, R.M.   "A Mass Transfer Model for a Twin-Screw Extruder".
                              Polym. Eng. Sci., 26, 647, 1986

DISTRIBUTION

No. of copies

Defence Science and Technology Organisation

Chief Defence Scientist
First Assistant Secretary Science Policy
Director General Science Resources Planning and Commercialisation
Director General Science and Technology Programs
Director General Space and Scientific Assessments
Assistant Secretary Science Corporate Management
Assistant Secretary Development Projects

} 1

Counsellor, Defence Science, London

Cnt Sht Only

Counsellor, Defence Science, Washington

Cnt Sht Only

Defence Science Representative, Bangkok

Cnt Sht Only

Scientific Adviser, Defence Research Centre, Kuala Lumpur

Cnt Sht Only

Scientific Adviser to Defence Central

1

Weapons Systems Research Laboratory

Director, Weapons Systems Research Laboratory

1

Chief, Ordnance Systems Division

1

Research Leader, Ballistic Weapons and Propulsion

1

Head, Propellants

1

Head, Propulsion Materials

1

Head, Engineering Support

1

Mr N. Ayres

1

Dr T. Nguyen

1

Mr B. Hamshere

1

Mr S. Odgers

1

WSRL-GD-28/90

Dr A. White	1
Mr P. Rawson	1
Mr P. Barry	1
Mr P. Whitehead	1
Mr A. Starks	1
Author	1

Materials Research Laboratory

Director, Materials Research Laboratory	1
Mr H. Billon	1

Libraries and Information Services

Librarian, Technical Reports Centre, Defence Central Library, Campbell Park	1

Document Exchange Centre,
Defence Information Services for:

Microfiche copying	1
United Kingdom, Defence Research Information Centre	2
United States, Defense Technical Information Center	2
Canada, Director Scientific Information Services	1
New Zealand, Ministry of Defence	1
National Library of Australia	1
Main Library, Defence Science and Technology Organisation Salisbury	2
Library, DSD, Melbourne	1
Library, Materials Research Laboratory	1

Australian Defence Force Academy	1
British Library, Document Support Centre	1
Department of Defence	
Director of Departmental Publications	1
Joint Intelligence Organisation (DSTI)	1
Australian Ordnance Council	
President	1
Australian Defence Industries	
Project REFA	
Project Manager	1
Mr A. Gangi	1
Ms J. Derrick	1
Mr I. Hird	1
Mulwala Explosives Factory	
General Manager	1
Mr A. Baker	1
Mr A. Wylie	1
Mr R. Sissons	1
Spares	10
Total number of copies	56

DOCUMENT CONTROL DATA SHEET

Security classification of this page : [UNCLASSIFIED]

1 DOCUMENT NUMBERS

AR Number :	AR-006-450
Series Number :	WSRL-GD-28/90
Other Numbers :	

2 SECURITY CLASSIFICATION

a. Complete Document :	Unclassified
b. Title in Isolation :	Unclassified
c. Summary in Isolation :	Unclassified

3 DOWNGRADING / DELIMITING INSTRUCTIONS

4 TITLE

BASIC RHEOLOGY AND ITS APPLICATION TO NITROCELLULOSE PROPELLANT
PROCESSING BY SCREW MIX-EXTRUDERS

5 PERSONAL AUTHOR (S)

R.C. Warren

6 DOCUMENT DATE

September 1990

7

7. 1 TOTAL NUMBER OF PAGES	46
7. 2 NUMBER OF REFERENCES	36

8 8. 1 CORPORATE AUTHOR (S)

Weapons Systems Research Laboratory

8. 2 DOCUMENT SERIES and NUMBER
General Document
28/90

9 REFERENCE NUMBERS

a. Task :	DST 87/183
b. Sponsoring Agency :	DSTO

10 COST CODE

11 IMPRINT (Publishing organisation)

Defence Science and Technology
Organisation

12 COMPUTER PROGRAM (S)
(Title (s) and language (s))

13 RELEASE LIMITATIONS (of the document)

Approved for Public Release.

Security classification of this page : [UNCLASSIFIED]

14 ANNOUNCEMENT LIMITATIONS (of the information on these pages)

No limitation

15 DESCRIPTORS

a. EJC Thesaurus Terms

Cellulose nitrate
Solid propellants
Rheology

b. Non - Thesaurus Terms

Propellant mixing
Screw mix-extruders

16 COSATI CODES

210902

17 SUMMARY OR ABSTRACT
(if this is security classified, the announcement of this report will be similarly classified)

(U) This document is intended to provide an introductory review of the rheology of propellant doughs and the propellant mixing process. The fundamental rheological quantities describing the flow of propellant doughs in mixing and extrusion are described, and the molecular factors affecting flow are discussed. Batch mixing is analysed in terms of the fundamental parameters which have been introduced, and a method of analysing screw mix-extrusion in a similar way is suggested.